VNU Journal of Science: Mathematics – Physics, Vol. 32, No. 4 (2016) 45-51

Magnetization and Magnetoresistance of Particulate Sr_2FeMoO_6 Samples Prepared via Sol-gel Route and Heat Treatment in H_2/Ar Atmospheres

Le Duc Hien[1,2], Dao Thi Thuy Nguyet[1], Luong Ngoc Anh[1], To Thanh Loan[1], Nguyen Phuc Duong[1,*], Ta Van Khoa[2], Than Duc Hien[1]

[1]*International Training Institute for Materials Science (ITIMS), Hanoi University of Science and Technology, 1 Dai Co Viet, Hanoi, Vietnam*

[2]*Technology Institute–General Department of Defense Technology, Duc Thang, North Tu Liem, Hanoi, Vietnam*

Received 10 November 2016
Revised 29 November 2016; Accepted 28 December 2016

Abstract: Double perovskite Sr_2FeMoO_6 samples were prepared via sol-gel route followed by heat treatment in reduce gas atmosphere of H_2/Ar (10 vol.% H_2) at 900–1100°C for 8 hours. All the samples contain the main phase Sr_2FeMoO_6 with tetragonal structure (space group *I*4/*m*) and a certain amount of secondary phase $SrMoO_4$ with contents being dependent on annealing temperature. Magnetic properties of the samples were investigated by means of vibrating sample magnetometer (VSM) in temperature range 80–450 K and in magnetic fields of ± 10 kOe. Their magnetoresistance in applied fields of ± 10 kOe was also studied at room temperature. The magnetization data were discussed based on the influence of impurity phase and cation antisite disorder parameter. The magnetoresistance results were analyzed based on the models of spin–dependent electron scattering and electron tunneling through grain boundaries.

Keywords: Sr_2FeMoO_6, sol-gel, antisite disorder, magnetization, magnetoresistance.

1. Introduction

Sr_2FeMoO_6 (SFMO) belongs to the double perovskite family with half-metallic ground states in which conduction electrons are fully spin polarized and have ferromagnetic transition temperatures well above room temperature (T_C > 400 K). Consequently, this material has tremendous potential for applications in the field of spintronics as spin injectors and tunneling magnetoresistance devices. The ideal structure of SFMO is a stacking of corner sharing FeO_6 and MoO_6 octahedral which alternate along three directions of the crystal and form the B and B' sublattices respectively, while the Sr cations occupy the vacant sites between octahedral. In the compound, the majority spin up channel with a band gap is formed by core spins of Fe^{3+} (S = 5/2) ions. On the other hand, the spin down t_{2g}

*Corresponding author. Tel.: 84-915527063
Email: duong@itims.edu.vn

states of Mo and Fe together with some small admixture of the O 2p states form a conduction band lying at the Fermi level exhibit a full negative polarization (P = -1) which is partially filled by $4d^1$ electrons of Mo^{5+}, whereas the e_g levels are empty [1]. The Mo and Fe t_{2g} states are coupled via hopping interaction mechanism. Because the available Fe t_{2g} state are purely spin down polarized the electron hopping can only occur when the localized Fe spin moments are ferromagnetically aligned. The overall magnetic moment is well described by the ionic model of an antiferromagnetic arrangement between Fe^{3+} core spin and the Mo^{5+} 4d spin leading to the net moment of 4 μ_B/f.u. However, in real materials a certain degree of antisite disorder (AS) often exists in which some of Mo ions occupy the Fe ion sites and vice versa hence the saturation magnetization is always lower than the predicted value. The magnetoresistance (MR) of this material in low applied magnetic fields is mostly explained by using models based on intergrain tunneling [2]. The magnitude of the MR effect depends on several important parameters such as AS, morphology and impurity phase $SrMoO_4$ [3-5]. Among different fabrication methods, sol-gel was employed to prepare SFMO samples [6-8]. By using sol-gel route, one can have more degrees of freedom to control the factors such as impurity phase, cation order, grain size and morphology which in turn modify the magnetic and electrical properties. In addition, this method opens way to incorporate this material in miniaturized devices.

In this work, we report the preparation of SFMO samples via sol-gel route and their magnetization and magnetoresistance data. The influence of percentage of AS and impurity phase content in the magnetic and MR properties were discussed.

2. Experiments

Synthesis

In the sol-gel procedure, aqueous solutions of $(NH_4)_6Mo_7O_{24}.4H_2O$, $Fe(NO_3).9H_2O$ and $Sr(NO_3)_2$ were prepared by dissolving stoichiometric amounts in deionized water. Firstly, solutions of $Fe(NO_3).9H_2O$ and $Sr(NO_3)_2$ were mixed together with citric acid until pH = 4. Solution of $(NH_4)_6Mo_7O_{24}.4H_2O$ was then added to obtain the final solution in which the molar ratios between metal ions are set according to the chemical formula of Sr_2FeMoO_6. The obtained solution was magnetically stirred at 80°C till the liquid turned to a gel. The gel was dried at 110°C for 24 h, then ground and heated at 500°C for 2 h. The powder portions were pressed into pellets and were annealed at high temperatures under stream of H_2/Ar mixed gas (15 vol.% H_2) for 8 h. The samples are denoted as D1, D2, D3 corresponding to annealing temperatures T_a = 900°C, 1000°C and 1100°C respectively.

Characterization

Synchrotron X–ray powder diffraction (SXRD) experiments were carried out at beamline SAXS of the Synchrotron Light Research Institute (Thailand) (λ = 1.54 Å). The diffraction data were analyzed using Rietveld method with the help of FullProf program [9]. The diffraction peaks were modeled by pseudo–Voigt function which is a sum of Gaussian and Lorentzian functions [10]. A standard of LaB_6 was used to determine instrument broadening. The refinement fitting quality was checked by goodness of fit (χ^2) and weighted profile R-factor (R_{wp}) [11]. The calculated results are accepted with χ^2 approaches 1 and R_{wp} is not higher than 10% [12].

Scanning Electron Microscopy SEM (JEOL JSM-7600F) was used to examine the particle size and morphology.

Magnetization curves were measured using a vibrating sample magnetometer VSM (ADE Technology–DMS 5000) in temperature range 80–450 K and applied magnetic fields up to 10 kOe.

Magnetoresistance was measured at room temperature in magnetic fields up to ± 10 kOe using standard four-probe technique.

3. Results and discussion

SXRD patterns of the samples are shown in Fig. 1. Beside the main phase SFMO (space group $I4/m$), impurity phase $SrMoO_4$ (space group $I4_1/a$) was detected in the samples. Rietveld quantitative analysis was performed to determine the fraction of each phase and the antisite disorder of Fe and Mo ions in B' and B sites in the main phase. Both $SrMoO_4$ fraction and antisite defect content decrease with increasing annealing temperature. At T_a = 1100°C the $SrMoO_4$ phase almost vanishes. The average crystallite sizes D of the samples were estimated by Scherrer formula applied to the widths of the diffraction peaks. The crystallite size appeared to slightly increase with T_a. The structural and phase parameters are given in Table 1. The particle size and morphology of the samples were investigated by SEM measurements. For demonstration, Fig. 2 presents the SEM images of the sample D2 at two magnification scales. It can be seen that from the early stage of the annealing process very small particles were formed with diameters comparable with the average crystallite size D determined from SXRD peak broadening. The small particles then interdiffused to form bigger clusters with sizes up to ~1 μm. Similar behaviors were observed for D1 and D3 samples.

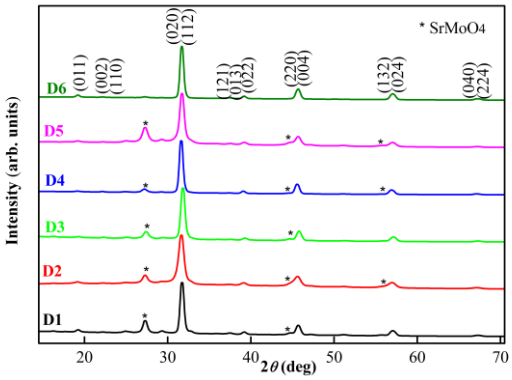

Figure 1. SXRD patterns of the Sr_2FeMoO_6 samples. The Miller indices of the main phase peaks and the peak positions of impurity are indicated.

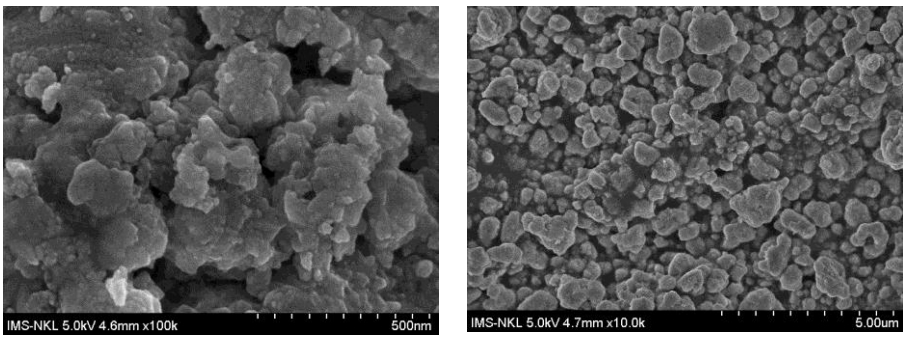

Figure 2. SEM images of sample D2 (enlarge scales: 500 nm (left) and 5 μm (right)).

Table 1. Rietveld quantitative analysis results for the samples and fitting quality (χ^2 and R_{wp})

Sample	*a*	*c*	*D*, nm	Antisite content ν, %	Sr_2FeMoO_6 wt %	$SrMoO_4$ wt %
D1	5.613(2)	7.928(4)	19.2(1)	40.6 ±1.2	94	6
D2	5.582(3)	7.898(8)	21.5(1)	21.5 ±1.4	90	10
D3	5.590(3)	7.863(1)	25.9(1)	13.1 ±1.3	98.4	1.6

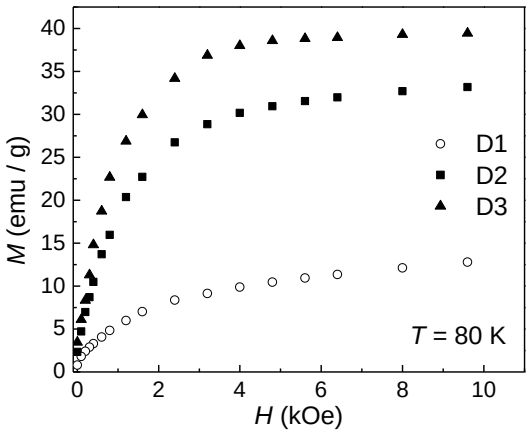

Figure 3. Magnetization curves at 80 K of samples D1, D2 and D3.

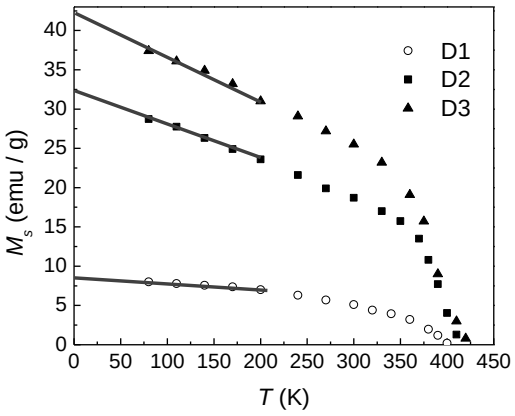

Figure 4. Temperature dependence of spontaneous magnetization M_s of samples D1, D2 and D3

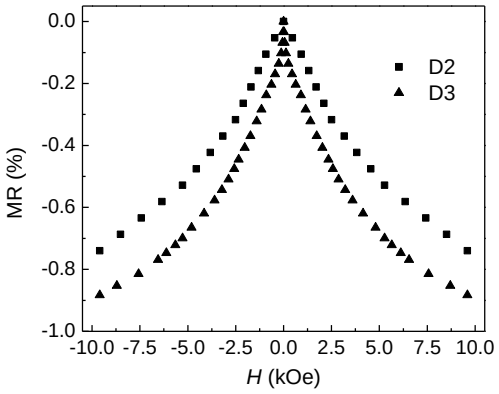

Figure 5. Room temperature magnetoresistance of samples D1, D2 and D3

Magnetization curves of the samples were measured in temperature range between 80 and 420 K in maximum field of 1 T. The magnetization curves at 80 K of three samples are shown in Fig. 3. For all cases, the magnetization increases steeply in the low-field part of the curve (below ~ 4 kOe) and then increases almost linearly with further increasing field. It is also noted that the derivative susceptibility in the high-field part decreases as we go from D1 to D3 samples. This behavior is closely related to the AS content. When Fe ions occupy B' sites, antiferromagnetic coupling between

Fe ions at B and B' is created which reduces the total magnetization and gives rise to an increase of high-field susceptibility. The spontaneous magnetization of the samples at each temperature was determined by extrapolating the linear part of the curve to zero field. The M_s values as a function of temperature are plotted in Fig. 4. It is seen that in temperature region up to about half of Curie temperature, M_s decreases linearly as temperature increases and then drops more drastically as temperature reaches T_C. This behavior is in consistent with the band structure calculation results reported by Erten et al. [13]. The M_s values at 0 K for the samples were determined by extrapolating the linear part of the M_s vs T curves down to zero Kelvin. From the derived spontaneous magnetization data, the net magnetic moments per formula unit at 0 K were calculated with correction for the non-magnetic $SrMoO_4$ impurity fraction in each sample. The results are shown in Table 2. It had been shown that the magnetic moment of SFMO samples is strongly dependent on the AS content ν [14, 15]. For perfectly order structure, the net moment per formula unit is equal to 4 μ_B and this value will decrease with increasing ν according to the formula $4(1 - 2\nu)\ \mu_B$. Based on the magnetic moments at 0 K of the samples, degrees of AS were calculated using the later formula and listed in Table 2. These values are in very good agreement with those determined via Rietveld analysis on the SXRD data.

Table 2. Magnetic parameters and antisite disorder content of D1, D2, D3 samples determined from magnetization data

Sample	M_s (emu/g)	m (μ_B/f.u.)	T_C (K)	Antisite content ν, %
D1	8.26	0.66	400	40.6
D2	30	2.52	411	18.5
D3	39.4	3.07	420	11.5

The Curie temperatures of the samples were determined as temperature at which M_s vanishes (Table 2). It is seen that T_C of sample D3 is ~ 420 K and it decreases slightly with increasing antisite contents (D2 and D1). This tendency is in agreement with experiments reported for bulk materials [16] and confirmed by band structure calculation and Monte-Carlo simulation [13].

In order to study the effects of the antisite disorder and impurity phase on the electrical properties of the materials, the resistivity at room temperature was measured which are 4.4 kΩcm, 28 Ωcm, 6 Ωcm for samples D1, D2 and D3, respectively. The metallic state remains in samples D2 and D3. The resistivity of the samples depends on both the content of the insulating $SrMoO_4$ phase and the degree of AS. Sample D2 has larger resistivity compared to sample D3 because it has larger amount of $SrMoO_4$. However, although sample D1 has lower content of impurity phase compared to D2 its resistivity is much higher. This can be due to the high level of AS (~ 40.6%) of sample D1 as indicated in Table 2 which largely decreases the conductivity of the main phase. Magnetoresistance of samples were measured at room temperature. For sample D1 magnetoresistance effect is not observable because of its very high resistivity. The MR results for D2 and D3 is shown in Fig. 5. For both cases, MR curve decreases faster in lower field range (H < 4 kOe) and decreases with further increasing field at lower rate. Similar MR behavior have been recorded for other double perovskite granular systems [14]. The MR in low-field range can be explained by intergrain tunneling mechanism. The samples can be described as a network of tunnel junctions whose electrodes are SFMO grains and they are separated by an insulating oxide layer [2]. At the coercive field the overall magnetization of the sample is zero and the magnetizations of the grains point randomly which constitute a higher resistance state compared to the low resistance state achieved above the saturation field, when all the magnetizations of neighboring grains are parallel. Hence, under the application of an external

magnetic field, the sample undergoes a resistivity decrease as the magnetization approaches saturation. According to this model MR effect of the samples should fully occur below the saturation field of ~4 kOe. The second component observed at higher field can be related with several phenomena such as the magnetic nature of the grain surface, the existence of magnetic impurities within the insulating grain boundaries, antisite disorder within the bulk grain, etc. The suppression of spin disorder in these locations under applied field gives rise to a decrease of the total resistivity. The MR values at H = 10 kOe were found to be -0.74% and -0.88% for samples D2 and D3 respectively, which are much lower than expected. The MR effect in this type of materials depends crucially on both the degree of spin polarization of electrons in the main phase and the composition of the grain boundary. The low MR values found in these samples are firstly attributed to the high levels of AS of SFMO phase which lowers the spin polarization of the conduction electrons. Theoretical prediction showed that with increasing the AS content ν the spin polarization at 0 K decreases from 100% with ν = 0 to approximately 40% and 30% with ν = 0.1 and 0.2, respectively [15]. Concerning the grain boundary structure, previous studies showed that the MR effect via the spin-dependent tunneling channel can be enhanced by introducing $SrMoO_4$ phase at grain boundaries in the SFMO samples [17,18]. However, at high temperatures, additional conduction channel created by spin-independent inelastic hopping through the localized states at grain boundaries becomes dominant which leads to a decrease of MR [17].

4. Conclusion

Sr_2FeMoO_6 samples were obtained by sol-gel route, using citric acid as a chelating agent. The amounts of impurity phase $SrMoO_4$ and antisite disorder can be controlled via annealing temperature and both were shown to be lessened with increasing T_a. Antisite disorder leads to a strong decrease of the net magnetic moment and a slight decrease of Curie temperature. Grain boundary structure can be modified by changing the amount of $SrMoO_4$ phase. Metallic state remains in the samples with $SrMoO_4$ phase of less than 10 wt.%. In addition, the conductivity of the main double perovskite phase depends strongly on the AS content. The MR values of samples D2 and D3 are low at room temperature in spite of their high Curie temperature which are attributed to the antisite disorder in the main phase. The presence of insulating impurity phase is also expected to have an impact on the MR effect. In order to control the magnetoresistance in these materials it is necessary to differentiate between the effects of antisite disorder of cations and impurity phase and this problem will be further studied in our future work.

Acknowledgments

The current work was financially supported by the Vietnam National Foundation for Science and Technology Development under Grant 103.02-2015.32.

References

[1] K. I. Kobayashi, T. Kimura, H. Sawada, K. Terakura, Room-temperature magnetoresistance in an oxide material with an ordered double-perovskite structure, Nature (London) 395 (1998) 677.

[2] D. Serrate, J. M. De Teresa, P. A. Algarabel, M. R. Ibarra, and J. Galibert, Intergrain magnetoresistance up to 50 T in the half-metallic $(Ba_{0.8}Sr_{0.2})_2FeMoO_6$ doubleperovskite: Spin-glass behavior of the grain boundary, Phys. Rev. B 71 (2005) 104409.

[3] M. García-Hernández, J. L. Martínez, M. J. Martínez-Lope, M. T. Casais, and J. A. Alonso, Finding Universal Correlations between Cationic Disorder and Low Field Magnetoresistance in FeMo Double Perovskite Series, Phys. Rev. Lett. 86 (2001) 2443.

[4] E. Burzo, I. Balasz, S. Constantinescu, I. G. Deac, Grain boundary effects in highly ordered Sr_2FeMoO_6, J. Magn. Magn. Mater. 316 (2007) e741.

[5] A. Gaur, G. D. Varma, Enhanced magnetoresistance in double poerovskite Sr_2MoFeO_6 through $SrMoO_4$ tunneling marries, Mater. Sci. Eng. B 143 (2007) 64.

[6] T. Takeda, M. Ito, S. Kikkawa, Preparation of magneto-resistive Sr2FeMoO6 through molybdic acid gelation, J. All. Comp. 449 (2008) 93.

[7] A. Calleja, X. G. Capdevila, M. Segarra, C. Frontera, F. Espiell, Cation order enhancement in Sr_2FeMoO_6 by water-saturated hydrogen reduction, J. Eur. Ceram. Soc. 31 (2011) 121.

[8] J. Raittila, T. Salminen, T. Suominen, K. Schlesier, P. Paturi, Nanocrystalline Sr_2FeMoO_6 prepared by citrate-gel method, J. Phys. Chem. Solids 67 (2006) 1712.

[9] S. Soontaranon and S. Rugmai, Small Angle X-ray Scattering at Siam Photon Laboratory, Chinese J. Phys. 50 (2012) 204.

[10] J. Rodriguez-carvajal, Structural Analysis from Powder Diffraction Data The Rietveld Method, Ec. Themat. Cristallogr. Neutrons 418 (1997) 73.

[11] D. Balzar, Voigt-function model in diffraction line-broadening analysis, Defects and Microstructure Analysis by Diffraction, International Union of Crystallography, Monograph on Crystallography (Oxford, UK: Oxford University Press, 1999) p. 94.

[12] L. B. McCusker, R. B. Von Dreele, D. E. Cox, D. Louër, and P. Scardi, Rietveld refinement guidelines, J. Appl. Crystallogr. 32 (1999) 36.

[13] O. Erten, O. Nganba Meetei, A. Mukherjee, M. Randeria, N. Trivedi, and P. Woodward, Theory of Half-Metallic Ferrimagnetism in Double Perovskites, Phys. Rev. Lett. 107 (2011) 257201.

[14] D. Serrate, J. M. De Teresa and M. R. Ibarra, Double perovskites with ferromagnetism above room temperature, J. Phys.: Condens. Matter 19 (2007) 023201.

[15] O. Nganba Meetei, O. Erten, A. Mukherjee, M. Randeria, N. Trivedi, and P. Woodward, Theory of half-metallic double perovskites. I. Double exchange mechanism, Phys Rev. B 87 (2013) 165104

[16] J. Navarro, J. Nogués, J. S. Muñoz, and J. Fontcuberta, Antisites and electron-doping effects on the magnetic transition of Sr_2FeMoO_6 double perovskite, Phys. Rev. B 67 (2003) 174416.

[17] K. Wang, Y. Sui, Influence of the modulating interfacial state on Sr_2FeMoO_6 powder magnetoresistance properties, Sol. State. Commun 129 (2004) 135.

[18] D.D. Sarma, E.V. Sampathkumaran, R. Sugata, R. Nagarajan, S. Majumdar, A. Kumar, G. Nalini, T.N. Gururow, Magnetoresistance in ordered and disordered double perovskite oxide, Sr_2FeMoO_6, Sol. State. Commun. 114 (2000) 465.